

Magnetic Liquid Patterns in Space and Time

Reinhard Richter¹, Bert Reimann¹, Adrian Lange², Peter Rupp¹, and Alexander Rothert¹

¹ Experimentalphysik V, Universität Bayreuth,
D-95440 Bayreuth, Germany

² Institut für Theoretische Physik, Universität Magdeburg,
D-39016 Magdeburg, Germany

Abstract. Macroscopic surface patterns of magnetic fluids are experimentally investigated for four different configurations of the liquid layer, and the orientation, homogeneity and temporal evolution of the magnetic field. Firstly the formation of surface undulations after a pulse-like application of the magnetic induction is examined. The wavenumbers measured for different magnetic induction are compared with the wavenumber of maximal growth predicted by linear stability analysis for the Rosensweig instability. Secondly, the formation of twin-peak patterns at the magnetic Faraday instability in an annular trough is reported. Thirdly, a ring of magnetic liquid spikes in a gradient magnetic field is periodically excited by an alternating magnetic field. The transition to spatiotemporal intermittency found in this way is characterized by power laws and their critical exponents. Eventually, we record the pinch-off of a magnetic liquid bridge by a high-speed camera. The temporal evolution of the neck radius is compared with results obtained theoretically via universal scaling functions.*

Molecules of liquids have in general an electric and magnetic dipole moment. Whereas these moments are of paramount importance for the chemical properties of the fluid, they are generically too tiny to have visible influence onto their fluid dynamical behaviour. This is different for liquids with artificially amplified magnetic moments. They have been synthesized for technical applications since the early 1960s [1]. These magnetic fluids (MFs) are colloidal suspensions of magnetic particles (e.g. from magnetite) in a carrier fluid like water or oil. They are protected from agglomeration due to van der Waals and magnetic forces by a layer of surfactants, or by ionic charges. The diameter of the suspended magnetic particles is in the range of 10 nm. Due to brownian motion the suspensions are then kept in a thermodynamically stable state. Their magnetic susceptibility ranges up to $\chi = 10$, which is much larger than the largest susceptibility for a natural fluid, liquid Oxygen. It has a χ of only 10^{-5} . Because of their huge susceptibility MFs are said to show super-paramagnetic behaviour. MFs offer the unique advantage to influence or even control their behaviour via an external magnetic field. E.g. they are drawn into an inhomogeneous magnetic field and thus can withstand gravity

* B. Kramer (Ed.): Adv. in Solid State Phys. **43**, pp. 789–799, 2003, Springer-Verlag, Berlin, Heidelberg 2003.

or forces due to pressure drop. In this way they have found widespread technical applications, ranging from rotary feed throughs in hard disc drives, to loud speakers (see Ref [2] e.g.).

From a scientific point of view MFs are attracting more and more interest essentially because of three reasons. Firstly, they serve as test liquids for electric and magnetic interactions, which are present also in common fluids. However, because they are difficult to measure they have also not taken into account in standard theory. These interactions are presently incorporated in a theory of electromagnetic fields in liquids, see e.g. Refs. [3] [4] [5]. Secondly, because the magnetic particles are rather large in comparison with atoms or even molecules, their suspension displays some granular character. Here the reversible formation of chains is one of several interesting subjects [6].

Thirdly the surface of MFs reacts to impressed magnetic fields by the spontaneous formation of macroscopic patterns. For static magnetic fields these structures are stable without any dissipation of energy. This is an important difference to the celebrated paradigms of pattern formation, like Rayleigh-Bénard convection, where the dissipation of energy is essential [7]. However, by modulation of the external field, dissipation and interesting spatio-temporal dynamics can be introduced to measure. In this article we will present some examples for surface structures in magnetic liquids, following a course from conservative to dissipative pattern forming systems. We start with the (static) Rosensweig instability, investigate its response to pulse-like and periodic modulation of parameters, observe spatiotemporal intermittency, and finally the disintegration of magnetic liquid bridges.

1 The Rosensweig Instability

In 1967 Cowley and Rosensweig first investigated the influence of a homogeneous magnetic field to a horizontally extended layer of magnetic fluid. When surpassing a critical value B_c of the magnetic induction, they observed a sudden transition between the flat surface and a hexagonal pattern of liquid crests [8,1]. Figure 1 gives a surface profile of this pattern by means of radioscopy [9].

A basic understanding of this instability can best be achieved via the dispersion relation for an semi-infinitely extended layer of inviscid MF [8,10]:

$$\omega^2 = gk - \mu \frac{(\mu_r - 1)^2}{\mu_r + 1} \frac{1}{\rho} H^2 k^2 + \frac{\sigma}{\rho} k^3. \quad (1)$$

Here ω denotes the frequency, k the wave number, H the strength of the external magnetic field, μ_r the relative magnetic permeability, $\mu = \mu_r \mu_0$ the magnetic permeability, and μ_0 the magnetic field constant. Moreover, ρ stands for the density and σ for the surface tension of the MF. Whereas the first and third term at the r.h.s. are due to gravity and capillary waves, respectively, which are common to all fluids, the second term is specific for MFs. By

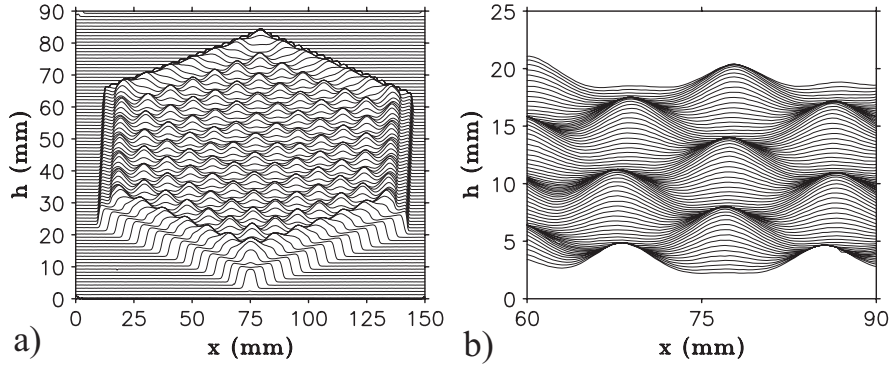


Fig. 1. Surface profile of the Rosensweig pattern at a magnetic induction of $B = 22.95$ mT (a) in a hexagonal shaped Teflon container of depth 4 mm for the MF EMG 909 from Ferrotec. Figure (b) displays a zoom of the center of the structure.

increasing H the dispersion relation can be tuned. At $H \approx 0.93 H_c$ Eq. (1) becomes non-monotonic, and at $H_c = [2(\mu_r + 1)/(\mu(\mu_r - 1)^2)\sqrt{\rho g \sigma}]^{1/2}$ the curve touches the $\omega = 0$ - line at the critical wave number $k_c = \sqrt{\rho g / \sigma}$. For $H > H_c$ Eq. (1) has a negative solution for a band of wavenumbers around k_c . Here $\Im(\omega) > 0$ and small disturbances from the basic state, which are proportional to $\exp[-i(\omega t - \mathbf{k} \cdot \mathbf{r})]$, begin to grow. It is important to stress, that with growing amplitude the range of validity of linear stability analysis is left.

The emerging stable hexagonal pattern and an unstable square pattern has been characterized in the vicinity of the bifurcation point by means of an energy minimization principle [11]. Figure 2 gives a scheme of the subcritical bifurcation diagram obtained in this way. In a recent and improved theoretical treatment a further unstable branch of liquid ridges has been predicted in the neighbourhood of the bifurcation point [12].

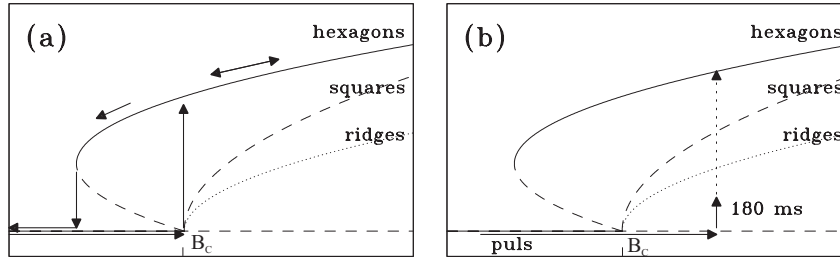


Fig. 2. Scheme of the bifurcation diagram in the vicinity of the bifurcation point B_c , as predicted by [11] and [12]. Figure (a) illustrates an adiabatic change of the control parameter B , (b) the consequences of a jump-like increase

Most experimentalists followed the pioneers [8] by varying the magnetic induction in a quasi static manner. By moving on the hysteretic course, sketched in Fig. 2(a), they were focusing on the nature of the stable pattern in the nonlinear regime [13,14]. The wavenumber observed in this way was found to be independent from the magnetic induction [8,13]. Unfortunately this result has been compared with the predictions of linear theory [15]. However, the final stable pattern, resulting from *nonlinear* interactions, does not generally correspond to the most unstable *linear* pattern.

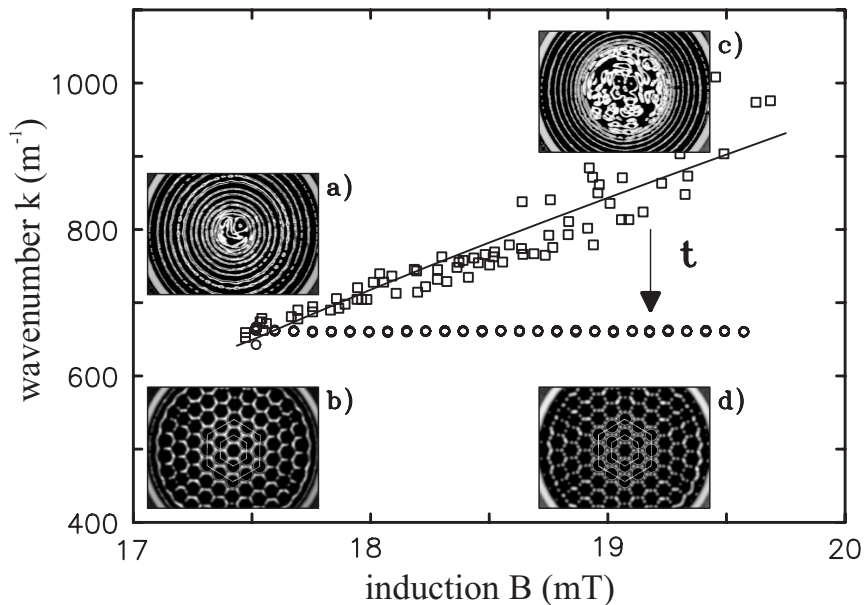


Fig. 3. Plot of the wavenumber k versus the magnetic induction B measured in a circular container of 120 mm diameter and 2 mm depth. The open squares give the experimental values extracted from the circular deformations, examples of which are given in the insets (a), (c). The solid line displays the theoretical results for the material parameters of the MF EMG 909 using $\mu_r \approx 1.85$ as a fit-parameter. The open circles denote the wavenumber of the final hexagonal patterns, example of which are shown in (b), (d), calculated via a fit of the central hexagonal structure. Figure taken from [16].

For a successful comparison with the predictions of linear theory [17], not fully developed crests of small amplitude are suitable. Due to the subcriticality of the prevailing bifurcation these are only accessible via a jump-like increase of the magnetic induction, as sketched in Fig. 2(b). The emerging transient magnetic liquid ridges of appropriate small amplitude are displayed in the insets (a) and (c) of Fig. 3. After this circular transient structures a

stable hexagonal pattern of Rosensweig crests evolves, as shown by the insets (b) and (d).

Next we focus on the quantitative experimental results displayed in Fig. 3, where the wavenumber k is plotted versus the magnetic induction B . Each open square denotes the wavenumber extracted from a picture taken 180 ms after the jump-like increase of the induction to $B > B_c$. The solid line gives the prediction of linear stability analysis, taking into account the viscosity and finite thickness of the layer of the fluid. Here the magnetic permeability μ_r has been used as the only fit parameter. The fitted value for μ_r differs by 2.8 % from the value given by the manufacturer. The almost linear increase both in experiment and theory is the main result. The inclination is predicted to depend on the viscosity of the MF, approximating zero only in the limit of infinite viscosity [17]. In contrast to this linear wavenumber dependence we find a constant behaviour for the wavenumber of the final hexagonal pattern, which is marked by the open circles. This measured constant value confirms the qualitative observations for the final pattern in [8,13]. The experimental data in Fig. 3 show convincingly the difference between the linear and nonlinear stages of the pattern forming process.

So far the viscous dissipation has been found to have measurable influence on the transient dynamics, but not on the final stable pattern. Increasing the role of dissipation can be done at will by combining MFs and periodic excitation. Depending on the range of the magnetic induction the product may be regarded as a periodically driven Rosensweig instability or a magnetic Faraday instability.

2 The Magnetic Faraday Instability

The Faraday instability belongs already to the most popular experimental configurations for the investigation of parametrically excited instabilities, structure formation and spatio-temporal chaos [7]. Operating the experiment with magnetic fluid instead of the commonly used water or silicon oil is adding further interesting aspects. Firstly, instead of shaking the container, the instability can also be driven by periodic modulation of the applied magnetic field (see Ref. [10,18–20], e.g.). Secondly, different orientations of the magnetic field with respect to the surface layer permit the realization of various symmetries [21,22]. Finally, the dispersion relation of MFs (1) can be tuned by the external magnetic field.

Experimentally, the non-monotonic dispersion relation was investigated by means of locally excited travelling waves in an annular channel [23], and in a circular container [24]. Due to the non-monotonicity up to three different wavenumbers can be excited with one single driving frequency. Which of the wavenumbers can actually be realized depends on the viscous dissipation in the bulk and in the bottom layer of the fluid [25]. For surface waves excited in a spatially homogeneous manner, the competition of the

different wavenumbers was predicted to result in the spontaneous formation of domain structures [26]. This symmetry-breaking process could be experimentally demonstrated in an annular channel excited by vertical vibration [27]. In the annulus a domain of standing subharmonic waves with the wavenumber $k_1 = 34$ and another domain with $k_2 = 46$ evolved. In addition to the predicted domain formation in space, for different parameters a domain formation in time could also be detected [27]: A standing wave pattern of wavenumber k_1 collapses spontaneously in the whole annulus, and gives way to a pattern with wavenumber k_2 . The latter however is not stable and forms a slowly shrinking domain, which finally vanishes in favour of k_1 . This cycle is repeated in an irregular manner.

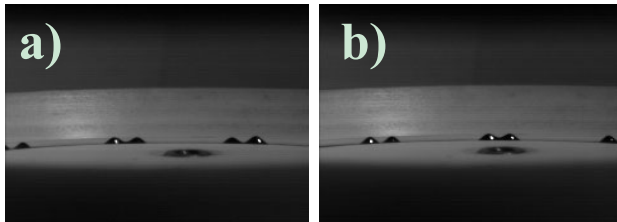


Fig. 4. Twin peak pattern in the non-monotonic regime of the dispersion relation. The time elapsed between picture (a) and (b) is one driving period

Recently, the competition between two different wavenumbers was found to be solved in a third way [28]. In the non-monotonic regime, for a magnetic field of $H = 0.98H_c$ and a driving frequency $\omega_D = 9.615\text{Hz}$ a novel pattern of twin peaks has been detected. Figure 4 displays two snapshots taken one driving period apart. One clearly unveils a subharmonic standing wave. Apparently, instead of two separated domains, a bi-periodic structure in space has been established. Both dominant wavenumbers of the twin-peak pattern are found to be situated on the non-monotonic dispersion curve [28].

3 Spatiotemporal Intermittency

Low dimensional chaotic dynamics of a single spike of MF has been investigated in experiment [29] and theory [30,31]. The next step is to tackle the problem of spatiotemporal complexity. In order to do so, a quasi one dimensional array of spike-oscillators is a natural choice. It can be realized by the magnetic Faraday instability in an annular trough filled with MF [27]. To facilitate a meaningful statistical evaluation of spatiotemporal complexity a high number of oscillators is most desirable. For a given circumference of the annulus the number of spike-oscillators is limited by the wavenumber of the nonlinear pattern. In case of a homogeneous magnetic field the wavenumber of the final nonlinear pattern was found to be independent from the magnetic induction, in agreement with Fig. 3.



Fig. 5. The MF EMG 901 trapped by the gradient magnetic field at the sharp edge of a pole shoe of an electro magnet. The diameter of the pole shoe is 40 mm

The number of oscillators could be increased by a decade, when utilizing an inhomogeneous magnetic field [32] and a MF with permeability $\mu_r = 4$. For this aim the flat ground state and the homogeneous field was sacrificed. Figure 5 presents a picture of the new ground state. A ring of up to 130 spikes is trapped by the field at the edge of a soft iron pole shoe of an electromagnet supplied by direct current of 1 A. The spikes can be excited periodically by applying in addition an alternating current I_{ex} . A CCD-camera takes pictures of the spatiotemporal dynamics phase-locked to the driving frequency. The 2D images are extracted in real time to 1D azimuthal scans along the ring of spikes. In Fig. 6(a) 500 of such scans of a laminar state are shown in space and time, where dark regions correspond to high amplitudes. Due to the stroboscopic recording the oscillations of the spikes can not be seen. For higher excitation amplitudes the laminar state becomes intermittent in space and time (Fig. 6(a)) and eventually chaotic (Fig. 6(c)).

As an order parameter for the transition to spatiotemporal intermittency (STI) we take the mean chaotic fraction γ , i.e. the ratio of chaotic regions to the length of the system. Its variation with the control parameter I_{ex} is shown in Fig. 7. Close to the onset of STI the mean chaotic fraction is expected to grow with a power law

$$\gamma \sim (I_{\text{ex}} - I_c)^\beta. \quad (2)$$

The solid line in Fig. 7 is a fit to our data, using I_c , β , and an offset representing background noise as adjustable parameters. The threshold value determined in this way is $I_c = 3.0 \pm 0.05$ A. The exponent $\beta = 0.3 \pm 0.05$ is in agreement with the exponent predicted for directed percolation, $\beta = 0.276486(8)$ [33], and thus corroborates the conjecture by Pomeau, that the transition to STI might be analogous to directed percolation [34]. To prove this conjecture more thoroughly we have investigated four further power laws, namely for the correlation length, the correlation time, the critical distribution of the laminar lengths and times. Three of four exponents turned out to be in agreement with the interpretation that chaotic domains spread within the laminar state according to the rules of directed percolation.

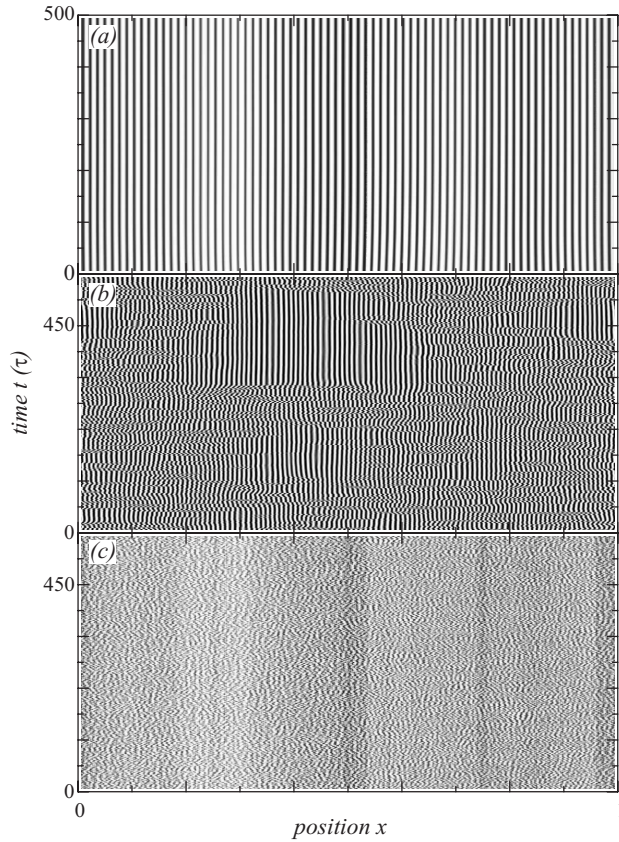


Fig. 6. Transition to spatio-temporal intermittency in a ring of 108 magnetic liquid spikes situated at the edge of a pole shoe. The Figure gives a series of stroboscopic azimuthal scans (a) in the laminar regime at $I_{ex} = 2.8$ A, (b) in the spatio-temporal intermittent regime at $I_{ex} = 3.0$ A, and (c) in the chaotic regime at $I_{ex} = 3.8$ A. The driving period $\tau = 1s/12.5$ is used to scale the time. Figure taken from [32]

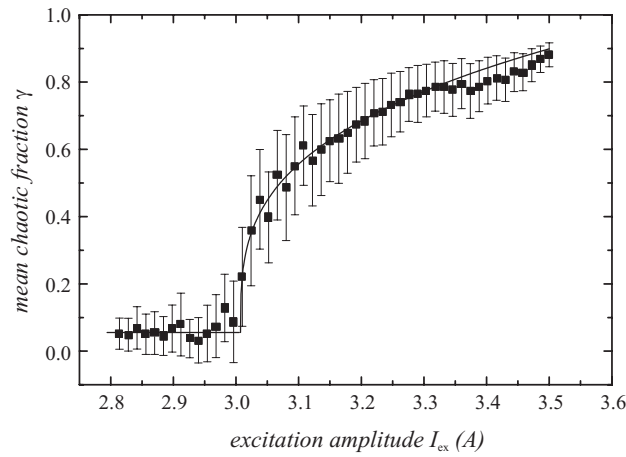


Fig. 7. The mean chaotic fraction γ vs. excitation amplitude I_{ex} . γ was extracted from 2000 excitation periods τ . The solid line is a power law fit. The error bars represent the statistical errors. Figure taken from [32]

4 Liquid Bridge Pinch-off

Liquid bridges in between a rotating shaft and a housing are one of the mayor industrial applications of MFs. Their stability and disintegration is apart from these applications also of fundamental interest for the investigation of drop formation. The early stage of the developing instability is described by classical linear stability analysis first conducted by Rayleigh [35]. In the last stage of the surface tension driven instability drop formation occurs. The surface- and flow structures immediately before drop pinch-off are described by universal scaling functions [36]. We have investigated whether this scaling laws for standard Newtonian liquids survive for the case of magnetic liquids subject to an axial magnetic field [37]. A magnetic liquid bridge is suspended in between the pole shoes of two electric magnets. Upon increase of the static magnetic field the bridge disintegrates. Figure 8 displays a sequence of frames during the rupture of the bridge.

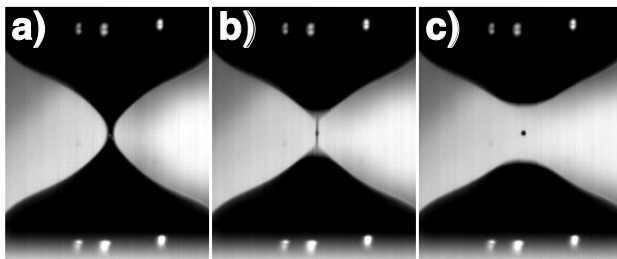


Fig. 8. Decay of a liquid bridge of magnetic fluid (APG J12 from Ferrofluidics) recorded by means of a high speed CCD-camera. The frames are taken at $t=0$ ms (a), 2ms (b), and 3ms (c). From [37].

During the last 3 ms before the rupture the measured neck radius is found to follow the equation

$$h_{\min} = u_{(a)s} \sigma (\nu \rho)^{-1} (t_0 - t). \quad (3)$$

Here $u_{(a)s}$ denotes the predicted dimensionless shrink velocities for the case of a symmetric or asymmetric solution, respectively, i.e. for Stokes- or Navier-Stokes flow. Moreover, t_0 denotes the time of pinch-off, σ the surface tension, ν the cinematic viscosity, and ρ the density. The measured value for u amounts to 0.068, which is close to the value $u_s = 0.071$ predicted by Papa-georgiou for the case of a viscosity dominated flow [38]. This is in agreement with the relatively large viscosity of the investigated magnetic fluid.

With decreasing neck radius, the flow is accelerated in the liquid thread. Eventually the Stokes approximation brakes down, and inertial terms become important. Such a transition is shown in Fig. 9 and could be observed for a glycerin-water mixture. It remains to be investigated, whether this transition can be observed as well for the case of MF. Tuning the magnetic field should shift the transition point, in analogy to recent findings for different viscosity of the glycerin-water mixture [40].

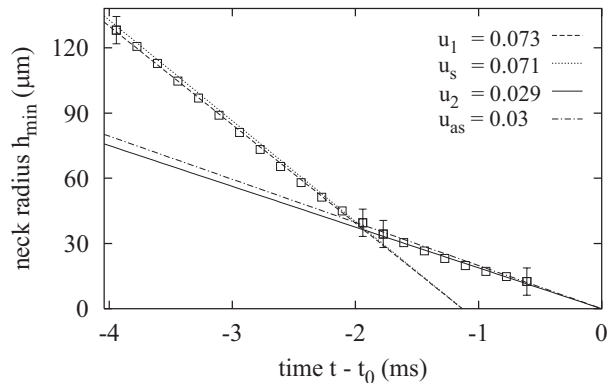


Fig. 9. The neck radius for the drop pinch-off of a glycerin-water mixture versus time. The dotted and the dashed line represent the theoretical prediction and a linear fit to the viscous dominated flow regime. The theoretical prediction and the linear fit for the Navier–Stokes flow are marked by the dash-dotted line and the solid line. From [39]

5 Conclusion

We have presented recent experimental efforts for a quantitative understanding of macroscopic surface patterns of magnetic fluids. Our three main outcomes are: For the two dimensional structures in a normal magnetic field, an almost linear dependence of the wavenumber of maximal growth on the magnetic induction. For a quasi one dimensional array of magnetic liquid spikes in a gradient magnetic field driven periodically we uncovered a transition to spatiotemporal intermittency. This transition yields some critical exponents known from directed percolation. For the decay of a magnetic liquid bridge the minimal neck radius was found to shrink with the velocity predicted for Stokes flow. — In this way pattern formation in 2D, 1D, and in the vicinity of a point of pinch-off has been investigated.

The projects have been supported in part by the ‘Deutsche Forschungsgemeinschaft’ under Grants En278/2, Re888/12 and Ri1054/1.

References

1. R. E. Rosensweig, *Ferrohydrodynamics* (Cambridge University Press, Cambridge, 1985).
2. B. Berkovski and V. Bashtovoy, *Magnetic fluids and applications handbook*, 1. ed. (Begell house, inc., New York, 1996).
3. M. I. Shliomis, *Sov. Phys. JETP* **34**, 1291 (1972).
4. M. Liu, *Phys. Rev. Lett.* 3580 (1993).
5. H. Müller and A. Engel, *Phys. Rev. E* **60**, 7001 (1999).

6. S. Odenbach., *Magnetoviscous Effects in Ferrofluids* (Springer, Berlin, Heidelberg, New York, 2002), Vol. m71.
7. M. C. Cross and P. C. Hohenberg, *Rev. Mod. Phys.* **65**, 870 (1993).
8. M. D. Cowley and R. E. Rosensweig, *J. Fluid Mech.* **30**, 671 (1967).
9. R. Richter and J. Bläsing, *Rev. Sci. Instrum.* **72**, 1729 (2001).
10. R. E. Zelazo and J. R. Melcher, *Fluid Mech* **39**, 1 (1969).
11. A. Gailitis, *J. Fluid Mech.* **82**, 401 (1977).
12. R. Friedrichs and A. Engel, *Phys. Rev. E* **64**, 021406 (2001).
13. J.-C. Bacri and D. Salin, *J. Phys. (France)* **45**, L559 (1984).
14. A. Boudouvis, J. Puchalla, L. Scriven, and R. Rosensweig, *J. Magn. Magn. Mater.* **65**, 307 (1987).
15. D. Salin, *Europhys. Lett.* **21**, 667 (1993).
16. A. Lange, B. Reimann, and R. Richter, *Magnetohydrodynamics* **37**, 261 (2001).
17. A. Lange, B. Reimann, and R. Richter, *Phys. Rev. E* **61**, 5528 (2000).
18. J.-C. Bacri, U. d'Ortona, and D. Salin, *Phys. Rev. Lett.* **67**, 50 (1991).
19. T. Mahr and I. Rehberg, *Europhys. Lett.* **43**, 23 (1998).
20. J. L. Hyun-Jae Pi, So-ycon Park and K. J. Lee, *Phys. Rev. Lett.* **84**, 5316 (2000).
21. J. C. Bacri, A. Cebers, S. Lacis, and R. Perzynski, *Phys. Rev. Lett.* **72**, 2705 (1994).
22. V. V. Mekhonoshin and A. Lange, *Phys. Rev. E* **65**, 061509 (2002).
23. T. Mahr, A. Groisman, and I. Rehberg, *J. Magn. Magn. Mater.* **159**, L45 (1996).
24. J. Browaeys, J.-C. Bacri, C. Flament, S. Neveu, and R. Perzynski, *Eur. Phys. J. B* **9**, 335 (1999).
25. H. W. Müller, *Phys. Rev. E* **55**, 6199 (1998).
26. D. Raitt and H. Riecke, *Phys. Rev. E* **55**, 5448 (1997).
27. T. Mahr and I. Rehberg, *Phys. Rev. Lett.* **81**, 89 (1998).
28. B. Reimann, T. Mahr, R. Richter, and I. Rehberg, *J. Magn. Magn. Mater.* **201**, 303 (1999).
29. T. Mahr and I. Rehberg, *Physica D* **111**, 335 (1997).
30. R. Friedrichs and A. Engel, *Eur. Phys. J. B* **18**, 329 (2000).
31. A. Lange, H. Langer, and A. Engel, *Physica D* **140**, 294 (2000).
32. P. Rupp, R. Richter, and I. Rehberg, *Phys. Rev. E* **67**, 0362XX (2003).
33. H. Hinrichsen, *Adv. Phys.* **49**, 815 (2000).
34. Y. Pomeau, *Physica D* **23**, 3 (1986).
35. J. W. S. Rayleigh, *Phil. Mag.* **34**, 145 (1892).
36. J. Eggers, *Rev. Mod. Phys.* **69**, 865 (1997).
37. A. Rothert and R. Richter, *J. Magn. Magn. Mater.* **201**, 324 (1999).
38. D. T. Papageorgiou, *Phys. Fluids* **7**, 1529 (1995).
39. A. Rothert, R. Richter, and I. Rehberg, *Phys. Rev. Lett.* **87**, 084501 (2001).
40. A. Rothert, R. Richter, and I. Rehberg, *New J. Phys.* **5**, 59 (2003).